IS-PORTO 2023 PROCEEDINGS

Proceedings of the 8th International Symposium on DEFORMATION CHARACTERISTICS OF GEOMATERIALS Porto, 3rd - 6th September 2023

Stiffness moduli in triaxial tests on a loess-sand mixture

Matylda Tankiewicz[1#], *Magdalena* Kowalska[2]

[1]*Wrocław University of Environmental and Life Sciences, Department of Civil Engineering, Norwida 25, 50-375 Wrocław, Poland*

[2]*Silesian University of Technology, Department of Geotechnics and Roads, Akademicka 5, 44-100 Gliwice, Poland*

[#]*Corresponding author: matylda.tankiewicz@upwr.edu.pl*

ABSTRACT

Stiffness is one of the most important characteristics of geomaterials, and at the same time one of the most difficult to evaluate. It can be described by means of various stress-strain moduli, whose values strongly depend on the strain range and on the method of determination. The aim of the article is to evaluate and compare selected stiffness parameters (Young's modulus E and shear modulus G) of an anthropogenic soil on the basis of triaxial tests. The experiments were carried out on samples consisting of loess mixed with sand. Loess is a collapsible aeolian sediment with a high calcium carbonate content and so it is a very challenging material for geotechnical applications. The addition of sand improves its properties and increases its suitability for earthworks. The specimens were compacted with normal Proctor energy at the optimal water content, which ensured repeatability of the results. Standard triaxial tests (drained and undrained) were carried out at the effective confining stresses in the range of 50 – 350 kPa. The specimens' deformation was measured by means of external and local displacement transducers. Additionally, bender elements were used to assess the initial soil stiffness. The applied research methods allowed determination of the deformation characteristics in the range from very small to large strains. The stiffness moduli were assessed using different definitions and methods. It was confirmed that the stiffness of loess is improved by its proper compaction and addition of sand, when compared to the results available in literature for natural loesses.

Keywords: stiffness; loess; triaxial test; bender elements; stiffness degradation curve.

1. Introduction

Soil stiffness is defined as the relation between the stress and strain tensors at a specific point. It is one of the most important geomechanical characteristics, because it determines the behaviour of soil subjected to loading. Its proper description is crucial in addressing many geotechnical design problems, such as foundations, retaining walls, road embankments, etc, at every stage of the engineering structure's life (design, execution, monitoring, improvement or demolition). In constitutive modelling it is described with a stiffness matrix and constitutes one of the most important and distinctive features of a model. In practice, stiffness is treated as a material parameter (a stiffness modulus) that is calculated as a gradient of a stress-strain curve. Due to the complicated nature of soils, the modulus' value depends on several factors, including the current stress and strain conditions, the loading history and loading velocity, the soil's structure, the saturation ratio, etc. As there are no well-defined common guidelines for the selection of particular test methods, this causes great difficulties in engineering practice. In the following sections the definitions of various stiffness moduli are given with indication of the method of their estimation. Practical examples are presented and compared based on results of triaxial tests on a chosen silt-sand mixture.

A silty soil has been chosen for experiments due to the limited data available in the literature for this type of material. The loess soil considered is an aeolian sediment with a high calcium carbonate content. It is common all over the world and is very challenging for geotechnical applications. In Poland extensive deposits can be found in the south. They form a part of the northern European Loess Belt, which extends from the United Kingdom through Belgium, the Netherlands, Germany, Poland, Ukraine and into Russia (Haase et al. 2007). A typical characteristic of natural loess is its collapsible structure i.e. significant volume reduction under load or due to an increased water content. The assessment of stiffness characteristics of undisturbed loess has been carried out by e.g. (Młynarek et al. 2015, Ng et al. 2017a, Rinaldi et al. 2007, 2001, Song et al. 2017, Wang et al. 2012, Zhong and Liu 2012). It has been shown that the natural structure and degree of saturation (water content/suction) are of particular importance among other factors influencing stiffness, as the sediments are usually unsaturated and slightly cemented, with honeycomb structure. To avoid the problems with collapsibility, in earthworks, the loess usually gets compacted and/or mixed with various additives. Investigations into the stiffness properties of compacted loess were carried out, among others, by (Chindaprasirt et al. 2022, Kim and Kang 2013, Ng et al. 2017b, Wang et al. 2021, 2022). Several researchers concentrated on chemical stabilisation, e.g. (Ghadakpour et al. 2020, Gu and Chen 2020, Sokolovich and Semkin 1984). Very few papers refer to loess improved by addition of coarser fraction (e.g. sand), which is one of the simplest solutions.

This paper evaluates and compares selected stiffness parameters i.e. Young modulus E and the shear modulus

G based on the results of standard triaxial tests. The test samples were compacted at optimum water content with normal Proctor energy to ensure repeatability of the results. The experiments were carried out on saturated specimens at the effective confining stresses of 50, 200 and 350 kPa. Bender elements were used to assess the initial soil stiffness. Usually, authors focus on a particular type of modulus and methodology. In this research, various definitions of the moduli were used and their values were evaluated in the drained and undrained tests at different strain ranges. The obtained results were compared with each other and with the data available in the literature for other similar soils.

2. Definitions of stiffness moduli

The most commonly used stiffness characteristics are the Young's modulus E (sometimes called simply 'elastic modulus') and the Poisson's ratio ν. They theoretically are relevant in unconfined compression tests, where the intermediate and minimum principal stress tensor components are equal to zero. In a general sense, E and ν are calculated using the equations:

$$E = \frac{\Delta\sigma'_v}{\Delta\varepsilon_v} \tag{1}$$

and

$$\nu = -\frac{\Delta\varepsilon_h}{\Delta\varepsilon_v} \tag{2}$$

where $\Delta\sigma'_v$ and $\Delta\varepsilon_v$ are the increments of axial (vertical) effective stress and strain, correspondingly, and $\Delta\varepsilon_h$ is the increment of strain in the direction perpendicular to the loading (horizontal).

The uniaxial state of stress is easy to apply in the laboratory and reflects well the functioning of steel or concrete elements in construction, but it hardly ever occurs in a real subsoil subjected to loading. Additionally, unconfined mechanical tests are often infeasible - e.g. for coarse uncemented soils.

In geotechnics much more preferred are triaxial tests where the specimens are confined (ISO 17892-8:2018, ISO 17892-9:2018). Triaxial test data are the basis for many constitutive models used in practice (e.g. of the critical state type). Their results are usually presented in the form of stress and strain tensor invariants: effective or total mean stress p' or p, effective or total stress intensity q' or q, volumetric strain ε_{vol} and strain intensity ε_s. In a classical triaxial compression test the applied state of stress is axisymmetric, which means that the equations reduce to these very simple forms:

$$p = \frac{1}{3}(\sigma_1 + 2\sigma_3) \tag{3a}$$

$$p' = \frac{1}{3}(\sigma'_1 + 2\sigma'_3) \tag{3b}$$

$$q = q' = \sigma_1 - \sigma_3 = \sigma'_1 - \sigma'_3 \tag{4}$$

$$\varepsilon_{vol} = \varepsilon_1 + 2\varepsilon_3 \tag{5}$$

$$\varepsilon_s = \frac{2}{3}(\varepsilon_1 - \varepsilon_3) \tag{6}$$

where: σ_1, σ_3, σ'_1, σ'_3, ε_1, ε_3 are the total maximum, total minimum, effective maximum and effective minimum principal stresses, and the maximum and minimum principal strains, respectively. The description also employs the shear stress τ and shear strain γ, which may be calculated from equations:

$$\tau = \frac{1}{2}(\sigma_1 - \sigma_3) = \frac{1}{2}q \tag{7}$$

$$\gamma = \varepsilon_1 - \varepsilon_3 = \frac{3}{2}\varepsilon_s \tag{8}$$

The elastic modulus evaluated in triaxial tests is calculated with Eq. (1), but necessarily with the indication of the effective confining stress at which it was evaluated. During the standard triaxial shearing stage, when the total confining stress is kept constant, the Young's modulus is usually calculated from the equation:

$$E = \frac{\Delta q}{\Delta\varepsilon_1} \tag{9}$$

It shall be noticed, that E values in an undrained test will be different than in a drained test due to the pore pressure changes influencing the axial effective stress. Hence, two types of elastic moduli ('drained' E' and 'undrained' E_u) are typically distinguished.

Another stiffness modulus used in geomechanics is the bulk (Helmholtz's) modulus K, which is determined from the volume change under isotropic compression. In triaxial tests it is defined as the ratio of the effective mean stress p' and the volumetric strain ε_{vol} increments under isotropic stress conditions:

$$K = \frac{\Delta p'}{\Delta\varepsilon_{vol}} \tag{10}$$

This can be easily achieved in a drained triaxial test when the specimen is subjected only to the changes in confining pressure ($\Delta q = 0$).

As the bulk modulus refers solely to the change in volume, a parameter describing the change in shape of the specimen must be included to complete the description of soil deformation. This is called shear (Kirchoff's) modulus G and is defined as the ratio of shear stress τ and shear strain γ in the conditions of simple shearing i.e. with no normal stress and strain tensor components and with no volume change ($\Delta p' = 0$, $\Delta\varepsilon_{vol} = 0$):

$$G = \frac{\Delta\tau}{\Delta\gamma} \tag{11}$$

The true simple shear can be simulated only in a simple shear apparatus. However, the test results are difficult to interpret due to the boundary effects (Chang et al. 2014). Additionally, this procedure has not been regulated by any European standard and such apparatus is still quite rare in the geotechnical laboratories. This is why the evaluation of the shear modulus is usually performed in triaxial tests using equation:

$$G = \frac{\Delta q'}{3\Delta\varepsilon_s} \tag{12}$$

To avoid the influence of the volumetric strain on the G value, the test may be conducted as undrained. In such a case, ε_s corresponds to ε_1 and G to one third of elastic ('undrained') modulus E. This approach however does not meet the $\Delta p' = 0$ condition.

The last stiffness modulus that is used in practice is the constrained (oedometric) modulus M calculated as the ratio of the vertical effective stress σ'_v and strain ε_v in the conditions of uniaxial state of strain (i.e. at constrained lateral deformations):

$$M = \frac{\Delta\sigma'_v}{\Delta\varepsilon_v} \tag{13}$$

It simulates well the behaviour of a shallow and thin compressible soil layer subjected to a load distributed uniformly over a large area. It shall be remembered that even though the definitions of the Young's modulus and oedometric modulus seem similar, the values of the moduli and their dependence on stress are completely different due to the different stress-strain conditions.

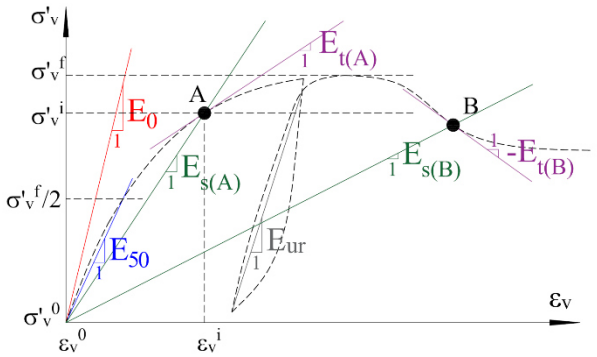

Figure 1. Definitions of the specific cases of the Young's moduli E: tangent E_t, secant E_s, initial E_0, secant at 50% of the ultimate stress E_{50} and unloading-reloading modulus E_{ur}.

All the moduli may be calculated as secant or tangent. In Fig. 1 an example of the Young's secant E_s and tangent E_t moduli are shown at two points, A and B. The secant moduli are calculated based on increments of stress and strain, most often referred to the initial value at the particular stage of the test (e.g. at point A: $\Delta\sigma_v = \sigma_v^i - \sigma_v^0$). The tangent moduli, on the other hand, are usually calculated based on the previous ($^{i-1}$) and the next ($^{i+1}$) reading relative to the specific point (e.g. $\Delta\sigma_v = \sigma_v^{i+1} - \sigma_v^{i-1}$).

As the soil behaviour is strongly nonlinear and depends on the loading history - the values of the moduli depend on the current values of the stress and strain (compare e.g. the moduli $E_{s(A)}$ and $E_{s(B)}$ in Fig. 1) and on the preconsolidation ratio OCR. It is well known that the soil stiffness becomes smaller the larger the strain is (Burland 1989, Viggiani and Atkinson 1995) and that, depending on the strain range, various methods of strain measurements must be applied to maintain the accuracy (Atkinson and Sallfors 1991, Atkinson 2000). Dynamic methods (bender elements, resonant columns, seismic *in situ* techniques) are used for very small strain levels $< 10^{-5}$, local (on-specimen) gauges for small strains in the order of 10^{-6} - 10^{-2} and conventional gauges for large strain levels i.e. $> 10^{-3}$. It may be noticed that in triaxial compression tests the secant modulus will always stay positive, while the tangent modulus will decrease to zero at the ultimate state (maximum q) and will further become negative if the soil softens (see point B in Fig. 1).

In constitutive modelling (e.g. the HS-Small model by (Benz 2006)) three characteristic parameters are often defined to represent the strong nonlinearity of stiffness (see Fig. 1):

- the initial (maximum) modulus (with subscript '0') denoting the stiffness value in the very small strain range ($< 10^{-5}$),
- the secant modulus established for 50% of the ultimate stress intensity q_f (with subscript '50') in initial loading stage,
- the unloading/reloading modulus (with subscript 'ur'), which is supposed to describe the mean secant stiffness at unloading and reloading at engineering strains ($\varepsilon_l \approx 10^{-3}$) - e.g. for simulation of an excavation and refilling (preconsolidation).

While the tangent and secant moduli in the small and large strain ranges may be determined in triaxial tests with the use of local and external strain transducers, the determination of the initial moduli requires a triaxial cell equipped with the bender elements (BE). BE tests provide a straightforward measurement of the shear modulus G [kPa] based on the shear wave velocity V_s [m/s] and the current bulk density of soil ρ [g/cm^3]:

$$G_0 = \rho V_s^2 \tag{14}$$

It is assumed that the strains generated by the passage of the shear wave are very small - less than 0.001% (Dyvik and Madshus 1985) and that the soil behaves in this strain range as a linearly elastic material. For an isotropic soil the initial Young's modulus E_0 may be then assumed as equal to:

$$E_0 = 2G_0(1 - \nu) \tag{15}$$

The Poisson's ratio in an undrained triaxial test is equal to 0.5, but in a drained test it shall be evaluated based on the velocity of the compression wave V_p (Richart et al. 1970):

$$\nu = \frac{\frac{1}{2}\left(\frac{V_p}{V_s}\right)^2 - 1}{\left(\frac{V_p}{V_s}\right)^2 - 1} \tag{16}$$

3. Material and methods

The study was carried out on loess from the Sudety forelands deposit in west-southern Poland (Lower Silesia). Loess in this area occurs in several separated "islands" with various thicknesses and properties (Krawczyk et al. 2017). The considered deposit is located in the Trzebnica Hills area in the neighbourhood of the city of Wrocław. The site has been investigated by many researchers in the field of geology and described, among others, by (Jary and Ciszek 2013, Jary and Krzyszkowski 1994, Krawczyk et al. 2017). In this area the loess deposits are mainly composed of interfluve and slope facies. Their thickness is typically 4 - 6 m and the soils usually contain high amounts of sand and clay fractions. Organic matter content is approx. 1% and calcium carbonate up to 5%.

Soil samples for testing were taken directly from a slope exposure. As it was intended to test remoulded samples, the material was taken without preserving the soil structure and moisture. The dried and powdered loess was mixed with medium quartz sand in the proportion

80% : 20% by weight. Sand, silt and clay fraction contents in the mixture are: Sa = 20.4%, Si = 63.4% and Cl = 16.1% respectively (ISO 17892-3:2015). The mixture is characterised by plastic limit PL = 19.9%, liquid limit LL = 25.5% (fall cone test), plasticity index PI = 5.6% (ISO 17892-12:2018) and specific gravity ρ_s = 2.66 g/cm^3 (ISO 17892-3:2015). The optimum water content in standard Proctor test (EN 13286-2:2010) is equal to 11,1% and the maximum dry density $\rho_{d.max}$ = 1,91 g/cm^3.

The triaxial samples were prepared by mixing dry soil with an amount of water corresponding to the optimum water content. After an overnight rest in an airtight container the mixture was placed in a cylinder with internal dimensions 70 mm in diameter and 140 mm in height and compacted in 3 layers with the standard Proctor energy. Using this method, the average density of 2,05 g/cm^3 ± 0,02 and initial void ratio of 0,44 ± 0,02 were obtained. The specimens were next subjected to monotonic triaxial compression tests (ISO 17892-9:2018, 2018). They were first saturated (at the back-pressure equal to 450 kPa), achieving a Skempton's B value ≥ 0.95, and then isotropically consolidated at the selected effective pressures σ'_3 = 50, 200 or 350 kPa. Next, the specimens were axially compressed maintaining the cell pressure constant. The rate of vertical displacement of the load frame was equal to 0.015 mm/min and 0.06 mm/min in the drained (CID) and undrained (CIU) conditions, respectively. Each test was conducted up to 15% of axial strain. The specimens' vertical deformation was measured by means of the external vertical displacement transducers. In two tests additionally the local sensors were used. The bender element tests were carried out on selected specimens at various consolidation pressures in the range of 10 - 400 kPa. The shear and compression wave velocities were assessed in time domain at the frequencies corresponding to the ratio L/λ equal to about 3.0, where L is the tip-to-tip distance between the bender elements and λ is the shear wave length. The first arrival time was assumed at zero after the first bump (point C according to (Lee and Santamarina 2005)). On this basis, the stiffness parameters of the tested material under different stress and strain conditions were determined.

4. Results and discussion

The values of the initial shear moduli, determined by means of bender element tests, are presented in Fig. 2 as a function of the mean effective stress p'_0 after isotropic consolidation. They increase non-linearly with the mean confining stress. The dependence can be expressed with the power function:

$$G_0 = 8.8611 \cdot (p'_0)^{0.5955} \quad (17)$$

The G_0 values were compared with the stiffness moduli results of other similar soils: compacted normally and overconsolidated loess (Sa = 5%, Si = 86%, Cl = 9%; initial bulk density 1.7 g/cm^3) tested by (Wang et al. 2021) and undisturbed Lanzhou loess wetted to about 16% of water content (Sa = 5%, Si = 85%, Cl = 10%, initial bulk density 1.45 - 1.75 g/cm^3) presented by (Song et al. 2017). These results are also shown in Fig. 2. The G_0 values for the improved loess obtained in this research are almost twice as large, which may be explained by the higher sand and clay content and much greater density. They are however lower than the values predicted with the model suggested by (Hassanipour et al. 2011) for well compacted sand-clay mixtures with Sa ≤ 60% (see Fig. 2).

For the Poisson's ratio ν, no significant dependence on pressure was observed, but a higher scatter was noticed at lower pressures, which might have been caused by worse contact between the soil and the bender elements. The average ν value is equal to 0.465, indicating nearly undrained conditions during the bender element testing. The elastic initial modulus E_0 may be roughly estimated as equal to 2.9 G_0. Its values are presented in Fig. 3. They also increase with the mean confining stress and the dependence may be described with the formula:

$$E_0 = 26.4097 \cdot (p'_0)^{0.5914} \quad (18)$$

As there are no special tests available to determine the values of the initial elastic modulus directly (other than its calculation based on Eq. (15)), there is little available data in literature for loess and silty soils to compare.

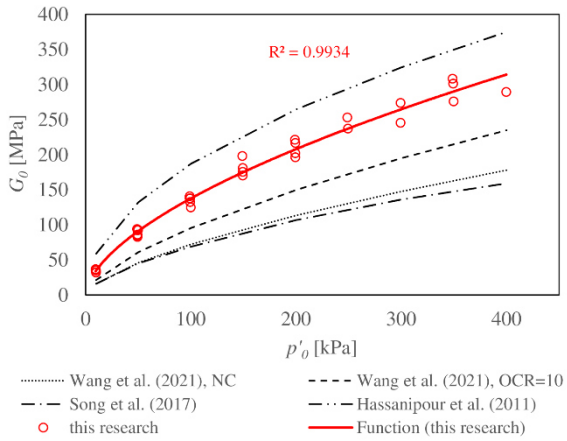

Figure 2. Dependence of the modulus G_0 on the mean stress p'_0.

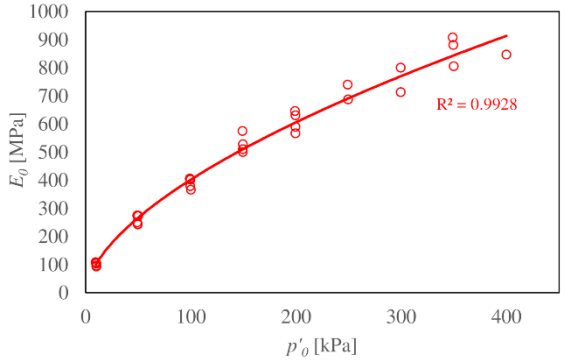

Figure 3. Dependence of the modulus E_0 on the mean stress p'_0.

The values of G and E in the intermediate and large strain ranges were determined on the basis of the monotonic triaxial tests. The stress-strain behaviour of all the tested specimens in the q - ε_1 space is shown in Fig.

4. In this and subsequent figures the results of the particular specimens are indicated by the confining effective stress in kPa (σ'_3 = 50, 200 or 350) and drainage conditions during the shearing stage (CID or CIU). The degradation of the secant and tangent shear and elastic moduli are presented in Fig. 5 and Fig. 6, respectively. To eliminate the influence of the mean effective stress, the values of the moduli were divided by the initial ones: G_0 calculated from Eq. (17) and E_0 derived from Eq. (18). This is one of the most commonly used types of normalisation for G modulus (Vardanega and Bolton 2013). Although in literature the E modulus is rather normalised with p'_0, it was decided to use the same type of normalisation for both the stiffness moduli for better comparison. The on-specimen displacement transducers were used in the 50/CID and 350/CID tests and results based on local sensors were plotted separately. It may be noticed that the soil stiffness assessed by means of the local transducers is higher than for external ones, which is related to the differences in their sensitivity and range.

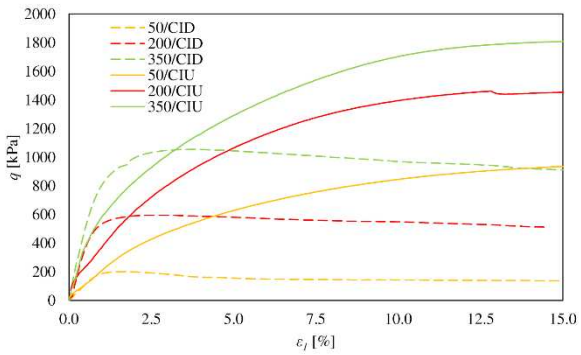

Figure 4. Shear characteristics of the tested specimens.

As is visible in Fig. 4 the behavior of the soil depends strongly on the drainage conditions. In the drained tests the mixture is initially showing higher stiffness but then, at the maximum dilatancy, it is yielding after reaching the peak strength at relatively small strain. In the undrained tests, the specimens exhibit continuous increase of the stress intensity without reaching any peak value until 15% axial strain. The strain at which the G/G_0 or E/E_0 degradation curves in the drained test intersects and falls below the undrained curve increases with the confining stress. For example, the secant G/G_0 at σ'_3 = 50 kPa in the CID test (Fig. 5a) decreases to the value observed in the CIU test at γ = 1.2%, while at σ'_3 = 350 kPa it happens at γ = 4.8%. This seems to be connected with the volume changes in CID tests, which are not allowed for in the calculation of G modulus - initially, at small shear strain, as the specimen contracts, it becomes stiffer and as it dilates - softer than in the undrained test with no volume changes. It may be also noticed that in the strain range above 1% in the drained tests for higher confining effective stresses the normalized stiffness values are higher and in undrained tests the relationship is reversed. This is probably the effect of the preconsolidation stress applied to the specimens during their preparation. To confirm that, further tests (e.g. oedometric) need to be conducted.

As expected (see e.g. (Gasparre et al. 2014)), the tangent moduli are generally smaller than the secant moduli and show small negative values at very large strains. To provide a better illustration of this trend, Fig. 7 shows a comparison of the normalised elastic moduli for the specimen 350/CID (based on the local sensors). The values of the tangent moduli are strongly influenced by the smallest change in the readings - this is why some scatter at the small strains is observed.

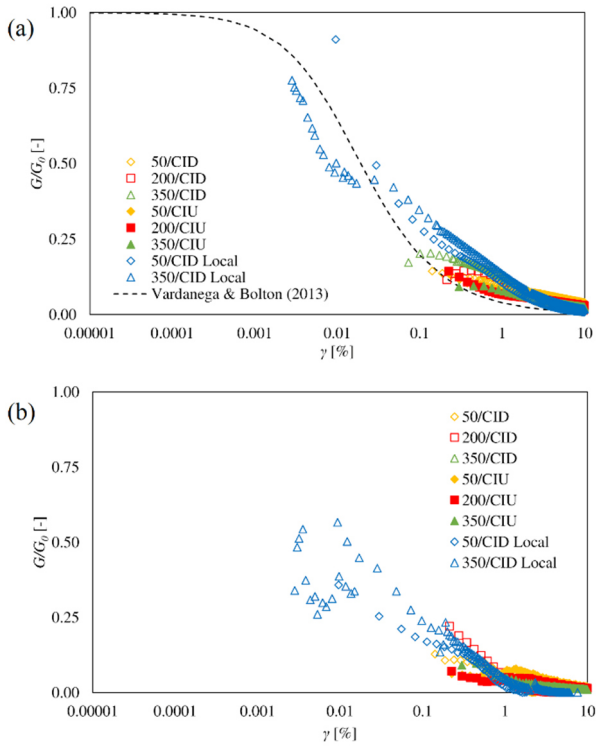

Figure 5. Degradation curves of the normalised shear modulus G/G_0: (a) secant; (b) tangent.

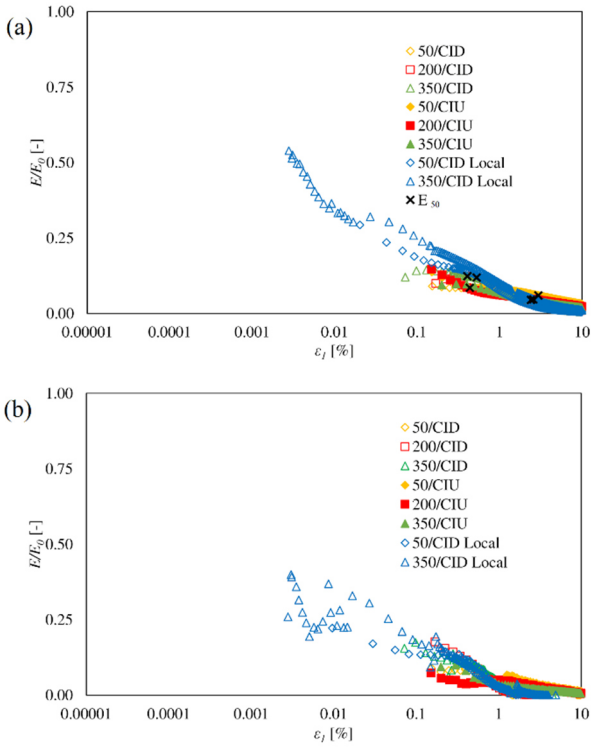

Figure 6. Degradation curves of the normalised shear modulus E/E_0: (a) secant; (b) tangent.

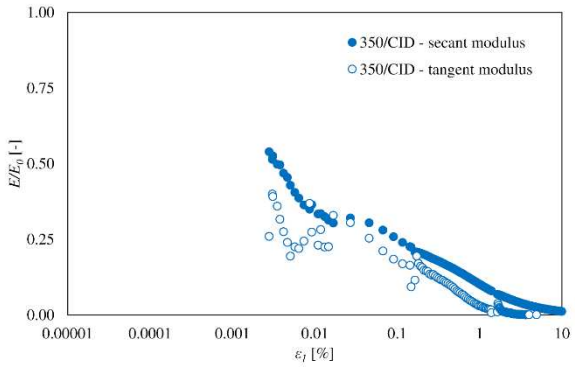

Figure 7. Exemplary degradation curves of the normalised elastic secant and tangent modulus.

Many theoretical and empirical formulas focusing on the description of the normalised secant modulus G/G_0 degradation curve can be found in the literature (see Soból et al. 2020). The non-linear stress-strain behaviour is most commonly described by various hyperbolic models based on the criterion proposed by (Darendeli 2001). Empirical equations and some further extensions based on this formula can be found e.g. in (Amir-Faryar et al. 2017, Oztoprak and Bolton 2013, Zhang et al. 2005). For fine soils, it is common to include the plasticity index *PI* as a variable in the equation. One of the best known proposals for cohesive soils in static applications was derived by (Vardanega and Bolton 2013) on the basis of a large set of literature results:

$$\frac{G}{G_0} = \frac{1}{\left(1+\frac{\gamma}{0.0022 \cdot PI}\right)^{0.736}} \quad (19)$$

It was used in Fig. 5a to compare with the results obtained in this research. It is obvious that this model does not adequately describe the behaviour of the compacted sand-loess mixture, showing too steep shear stiffness degradation with strain. For large deformations determined with external sensors, this relationship is closer, but for results from local sensors the inconsistency is large. This noncompliance may result from the very low colloidal activity (typical for loess) and, thus, from the fact that the plasticity index may be less descriptive of the soil type when compared to text-book fine soils. Proposing an individual empirical equation, however, requires further research.

As far as the E/E_0 degradation curve is concerned some theoretical relations can be found e.g. in (Atkinson 2000, Clayton 2011, Puzrin and Burland 1996). There are however practically no results for loess available in the literature to compare.

In practical applications (if the simple linear elastic-perfectly plastic Coulomb-Mohr constitutive model is to be used in the design) the civil engineers usually choose the E_{50} secant modulus. A summary of the established values is given in Table 1 and the corresponding points are marked in Fig. 6a. In the undrained tests the vertical strain at which E_{50} was established is equal to about 2.4 - 3.0%, while in the drained tests it is 0.4 - 0.5% (or even 0.2 - 0.4% if the local sensors are used). This explains the lower E_{50} values in the undrained conditions when compared to the drained ones. The results obtained for the undrained specimens are much higher than those obtained by (Capdevila and Rinaldi 2015) for recompacted loess with a much lower density and lower sand content. On the other hand, they are consistent with the results presented by (Zarei et al. 2022) for compacted loess with very similar density. This fact confirms again the great influence of compaction on the loess stiffness, and highlights the importance of indicating the drainage conditions expected in the analysed case.

Table 1. Values of the secant moduli E_{50}

Test	E'_{50} [MPa]	Test	E_{u50} [MPa]
50/CID	22.7/41.1*	**50/CIU**	16.0
200/CID	75.1	**200/CIU**	28.5
350/CID	100.9/142.3*	**350/CIU**	37.9

*values based on local sensors

5. Summary and conclusions

The paper presents the results of monotonic triaxial compression tests on a compacted loess-sand mixture. The results of shear and elastic moduli from small to large strains, for drained and undrained triaxial tests, as well as secant, tangent and initial moduli, are provided. The major conclusions are:

- The initial moduli G_0 and E_0 are correlated with the consolidation stress and can be easily described by a classical power function. The obtained values are higher than in other published researches, which is due to the higher clay and sand content and density. Addition of sand and optimum compaction are effective methods of loess improvement in terms of stiffness.
- The use of typical empirical relationships modelling the maximum soil stiffness and its degradation with strain may not give sufficiently good results for the compacted loess-sand mixture.
- The drainage conditions have a large influence on the soil stiffness in the range of intermediate and large strains. At smaller strains the stiffness (G and E moduli) of the loess-sand mixture is larger in drained conditions than in undrained, but later the degradation curves intersect and at large strains the undrained soil exhibits higher stiffness. The strain at which this interchange happens increases with the confining stress.
- Tangent stiffness moduli show higher variability at small strains as they are very sensitive to any changes in the slope of the stress-strain curve. Their values are smaller than the secant moduli - in drained tests after the mixture achieves the maximum stress intensity they fall below zero.
- The values of the specific secant 'engineering' moduli E_{50} are higher in the drained conditions. The use of local sensors, which are more reliable in the smaller strain range, produces even higher values.

Acknowledgements

The project presented in this article is supported by Wrocław University of Environmental and Life Sciences (Poland) as part of the program "Innovative Scientist" No. N060/0013/2021.

References

Amir-Faryar, B., Aggour, M.S., McCuen, R.H. "Universal model forms for predicting the shear modulus and material damping of soils", Geomech Geoengin, 12, pp. 60–71, 2017. https://doi.org/10.1080/17486025.2016.1162332

Atkinson, J., Sallfors, G. "Experimental determination of stress–strain–time characteristics in laboratory and in situ tests", In: Proceedings of the 10th ECSMFE, Florence, Italy, 1991, pp. 915-956. https://doi.org/10.1017/CBO9781107415324.004

Atkinson, J.H. "Non-linear soil stiffness in routine design", Géotechnique, 50, pp. 487–508, 2000. https://doi.org/10.1680/geot.2000.50.5.487

Benz, T. "Small Strain Stiffness of Soils and Its Numerical Consequences", PhD Thesis, Universitat Stuttgart, 2006.

Burland, J.B. "Ninth Laurits Bjerrum Memorial Lecture: "Small is beautiful"—the stiffness of soils at small strains", Can Geotech J, 26, pp. 499–516, 1989. https://doi.org/10.1139/t89-064

Capdevila, J., Rinaldi, V. "Stress-strain behavior of a heterogeneous and lightly cemented soil under triaxial compression test", Electronic J Geotech Eng, 20(6), pp. 6745-6760, 2015.

Chang, W.-J., Phantachang, T., Ieong, W.-M. "Evaluation of size and boundary effects in simple shear tests with distinct element method", 2014 World Congress on Advances in Civil, Environmental, and Materials Research, Busan, Korea, August 24-28, 2014.

Chindaprasirt, P., Sriyoratch, A., Arngbunta, A., Chetchotisak, P., Jitsangiam, P., Kampala, A. "Estimation of modulus of elasticity of compacted loess soil and lateritic-loess soil from laboratory plate bearing test", Case Stud Constr Mater, 16, e00837, 2022. https://doi.org/10.1016/j.cscm.2021.e00837

Clayton, C. R. I. "Stiffness at small strain: research and practice", Géotechnique, 61, pp. 5–37, 2011. https://doi.org/10.1680/geot.2011.61.1.5

Darendeli, M.B. "Development of a new family of normalized modulus reduction and material damping curves", PhD Thesis, The University of Texas at Austin, 2001.

Dyvik, R., Madshus, C. "Lab measurements of G_{max} using bender elements", In: Advances in the Art of Testing Soil under Cyclic Conditions, Detroit, USA, pp. 186–196, 1985.

European Committee for Standardization "EN 13286-2:2010 Unbound and hydraulically bound mixtures - Part 2: Test methods for laboratory reference density and water content - Proctor compaction", CEN/TC 227 "Road Materials", Brussels, 2010.

Gasparre, A., Hight, D. W., Coop, M. R., Jardine, R. J. "The laboratory measurement and interpretation of the small-strain stiffness of stiff clays", Géotechnique, 64, pp. 942–953, 2014. https://doi.org/10.1680/geot.13.P.227

Ghadakpour, M., Choobbasti, A.J., Kutanaei, S.S. "Experimental study of impact of cement treatment on the shear behavior of loess and clay" Arab J Geosci, 13(4), pp. 1-11, 2020. https://doi.org/10.1007/s12517-020-5181-7

Gu, K., Chen, B. "Loess stabilization using cement, waste phosphogypsum, fly ash and quicklime for self-compacting rammed earth construction", Constr Build Mater, 231, 117195, 2020. https://doi.org/10.1016/j.conbuildmat.2019.117195

Haase, D., Fink, J., Haase, G., Ruske, R., Pécsi, M., Richter, H., Altermann, M., Jäger, K.D. "Loess in Europe—its spatial distribution based on a European Loess Map, scale 1:2,500,000", Quat Sci Rev, 26, pp. 1301–1312, 2007. https://doi.org/10.1016/j.quascirev.2007.02.003

Hassanipour, A., Shafiee, A., Jafari, M.K. "Low-amplitude dynamic properties for compacted sand-clay mixtures", Int J Civ Eng, 9(4), pp. 255-264, 2011.

International Organization for Standardization "ISO 17892-3:2015 Geotechnical investigation and testing — Laboratory testing of soil — Part 3: Determination of particle density", Switzerland, 2015.

International Organization for Standardization "ISO 17892-8:2018 Geotechnical investigation and testing — Laboratory testing of soil — Part 8: Unconsolidated undrained triaxial test", Switzerland, 2018.

International Organization for Standardization "ISO 17892-9:2018 Geotechnical investigation and testing — Laboratory testing of soil — Part 9: Consolidated triaxial compression tests on water saturated soils", Switzerland, 2018.

International Organization for Standardization "ISO 17892-12:2018 Geotechnical investigation and testing — Laboratory testing of soil — Part 12: Determination of liquid and plastic limits", Switzerland, 2018.

Jary, Z., Ciszek, D. "Late Pleistocene loess–palaeosol sequences in Poland and western Ukraine", Quat Int, 296, pp. 37–50, 2013. https://doi.org/10.1016/j.quaint.2012.07.009

Jary, Z., Krzyszkowski, D. "Stratigraphy, genesis and properties of loess in Trzebnica brickyard, Southwestern Poland", Acta Univ Wratislav, 1702, pp. 63–83, 1994.

Kim, D., Kang, S.-S. "Engineering properties of compacted loesses as construction materials", KSCE J Civ Eng, 17, pp. 335–341, 2013. https://doi.org/10.1007/s12205-013-0872-1

Krawczyk, M., Ryzner, K., Skurzyński, J., Jary, Z. "Lithological indicators of loess sedimentation of SW Poland", Contemp. Trends Geosci, 6, pp. 94–111, 2017. https://doi.org/10.1515/ctg-2017-0008

Lee, J.S., Santamarina, J.C. "Bender Elements: Performance and Signal Interpretation", J Geotech Geoenvironmental Eng, 131, pp. 1063–1070, 2005. https://doi.org/10.1061/(ASCE)1090-0241(2005)131:9(1063)

Młynarek, Z., Wierzbicki, J., Mańka, M. "Geotechnical Parameters of Loess Soils from CPTU and SDMT", In: 3rd International Conference on the Flat Dilatometer DMT'15, Rome, Italy, 2015, pp. 481-489.

Ng, C.W.W., Baghbanrezvan, S., Sadeghi, H., Zhou, C., Jafarzadeh, F. "Effect of specimen preparation techniques on dynamic properties of unsaturated fine-grained soil at high suctions", Can Geotech J, 54(9), pp. 1310-1319, 2017a. https://doi.org/10.1139/cgj-2016-0531

Ng, C.W.W., Kaewsong, R., Zhou, C., Alonso, E.E. "Small strain shear moduli of unsaturated natural and compacted loess", Géotechnique, 67, pp. 646–651, 2017b. https://doi.org/10.1680/jgeot.16.T.013

Oztoprak, S., Bolton, M.D. "Stiffness of sands through a laboratory test database", Géotechnique, 63(1), pp. 54-70, 2013. https://doi.org/10.1680/geot.10.P.078

Puzrin, A.M., Burland, J.B. "A logarithmic stress–strain function for rocks and soils", Géotechnique, 46, pp. 157–164, 1996. https://doi.org/10.1680/geot.1996.46.1.157

Richart, F.E., Hall, J.R., Woods, R. "Vibrations of Soils and Foundations" Prentice-Hall Inc., Englewood Cliffs, USA, 1970.

Rinaldi, V., Claria, J.J., Santamarina, J.C. "The small-strain shear modulus (G_{max}) of Argentinean loess", In: 15th International Conference on Soil Mechanics and

Foundation Engineering, Istanbul, Turkey, 2001, pp. 495-498.
Rinaldi, V., Rocca, R.J., Zeballos, M. “Geotechnical characterization and behaviour of Argentinean collapsible loess”, Characterisation Eng Prop Nat Soils, 3, pp. 2259–2286, 2007. https://doi.org/10.1201/NOE0415426916.ch16
Soból, E., Gabryś, K., Zabłocka, K., Šadzevičius, R., Skominas, R., Sas, W. “Laboratory Studies of Small Strain Stiffness and Modulus Degradation of Warsaw Mineral Cohesive Soils”, Minerals, 10(12), 1127, 2020. https://doi.org/10.3390/min10121127
Sokolovich, V.E., Semkin, V.V. “Chemical stabilization of loess soils”, Soil Mech Found Eng, 21, pp. 149–154, 1984. https://doi.org/10.1007/BF01710605
Song, B., Tsinaris, A., Anastasiadis, A., Pitilakis, K., Chen, W. “Small-strain stiffness and damping of Lanzhou loess”, Soil Dyn Earthq Eng, 95, pp. 96–105, 2017. https://doi.org/10.1016/j.soildyn.2017.01.041
Vardanega, P.J., Bolton, M.D. “Stiffness of Clays and Silts: Normalizing Shear Modulus and Shear Strain”, J Geotech Geoenvironmental Eng, 139, pp. 1575–1589, 2013. https://doi.org/10.1061/(ASCE)GT.1943-5606.0000887
Viggiani, G., Atkinson, J. H. “Stiffness of fine-grained soil at very small strains”, Géotechnique, 45, pp. 249–265, 1995. https://doi.org/10.1680/geot.1995.45.2.249
Wang, F., Li, D., Du, W., Zarei, C., Liu, Y. “Bender Element Measurement for Small-Strain Shear Modulus of Compacted Loess”, Int J Geomech, 21, 04021063, 2021. https://doi.org/10.1061/(ASCE)GM.1943-5622.0002004
Wang, R., Hu, Z., Ren, X., Li, F., Zhang, F. “Dynamic modulus and damping ratio of compacted loess under long-term traffic loading”, Road Mater Pavement Des, 23, pp. 1731–1745, 2022. https://doi.org/10.1080/14680629.2021.1924232
Wang, Z., Luo, Y., Guo, H., Tian, H. “Effects of initial deviatoric stress ratios on dynamic shear modulus and damping ratio of undisturbed loess in China”, Eng Geol, 143, pp. 43–50, 2012. https://doi.org/10.1016/j.enggeo.2012.06.009
Zarei, C., Wang, F., Qiu, P., Fang, P., Liu, Y. “Laboratory Investigations on Geotechnical Characteristics of Albumen Treated Loess Soil”, KSCE J Civ Eng, 26, pp. 539–549, 2022. https://doi.org/10.1007/s12205-021-1723-0
Zhang, J., Andrus, R.D., Juang, C.H. “Normalized Shear Modulus and Material Damping Ratio Relationships”, J Geotech Geoenvironmental Eng, 131, pp. 453–464, 2005. https://doi.org/10.1061/(ASCE)1090-0241(2005)131:4(453)
Zhong, Z., Liu, X. “Mechanical characteristics of intact Middle Pleistocene Epoch loess in northwestern China”, J Cent South Univ, 19, pp. 1163–1168, 2012. https://doi.org/10.1007/s11771-012-1123-1